

HIGH-ALTITUDE CIRRUS FROM LIDAR MEASUREMENTS OVER HEFEI (31.90°N,117.16°E) , CHINA

Jun Zhou , Xinlian Xue , Dong Liu

Anhui Institute of Optics and Fine Mechanics, Chinese Academy of Science, Hefei 230031, China, jzhou@aiofm.ac.cn

ABSTRACT

This paper presents structures and optical properties of high-altitude cirrus from 90 nights of lidar measurements at Hefei (31.90°N,117.16°E) , Anhui Province, China. Meteorological data from nearby radiosonde measurements are used to analyze the lidar observed results. A method for retrieving the transmittance of discontinuous high-altitude cirrus is also presented.

1. INTRODUCTION

Cirrus clouds are one of the most commonly occurring cloud types globally. They form in the upper part of troposphere, due to synoptic scale lifting, or as a result of moisture transport by deep convection[1]. Aircraft condensation trails also can spread to form cirrus. Cirrus clouds cover nearly 30% of the earth's surface. Because they absorb long-wave outgoing radiation from Earth surface and reflect incoming solar radiation, cirrus clouds play an important role in the Earth's radiation budget. Therefore, knowledge of geometrical and optical properties of the cirrus clouds is essential for climate models.

Ground-based lidar offers an excellent way to obtain high accurate cirrus data. So far, a number of authors have reported the lidar processing methods and observational results of the cirrus clouds [2-8]. However, up to now, there still are very few data sets of lidar observed cirrus clouds over the East Asia area.

This paper describes statistical characteristics of high-altitude cirrus from Mie lidar measurements at Hefei (31.90°N,117.16°E) , Anhui Province, China. Structures and optical properties of these cirrus are presented. Meteorological data from nearby radiosonde measurements are used to analyze the lidar observed results. Moreover, a method is presented, that permits determination of the transmittance for discontinuous high-altitude cirrus

2. MIE LIDAR

The Mie lidar is composed of a frequency doubled Nd:YAG laser transmitter, a receiving optics, a signal receiver and a data-acquisition. Table 1 lists main technical parameters of the lidar system.

Table 1. Specifications of the Mie lidar

LASER	Nd:YAG
Wavelength (nm)	532
Pulse energy (mJ)	180
Repetition rate (Hz)	10
Beam divergence (mrad)	0.5
Polarization purity(%)	98
RECEIVING OPTICS	
Telescope	Cassgrain
Diameter (mm)	250
Field of view (mrad)	1
Polarizer	CVIPBS-532-100
Pass band of Filter (nm)	0.3
SIGNAL RECEIVER	
PMT	H7680 / H7680-01
AMP	Philips 777
DATA ACQUISITION	
Type	GAGE1610
Time Bin (ns)	200
Accuracy	16-bit
Computer	WS-855A

3. MEASUREMENT AND DATA PROCESSING

The high-altitude cirrus clouds were simultaneously detected when the Mie lidar took regular measurements of tropospheric aerosol. For each nighttime measurement 10000 laser shots were fired to get one vertical profile of aerosol extinction coefficients.

These high-altitude cirrus mostly were thin cirrus, including some subvisual or threshold visible cirrus. Their optical attenuation is weak, the laser pulse can penetrate through the cirrus completely and the signal transition from the top of the cirrus to the clear air return can be detected. Thus their effect on retrieving aerosol extinction above the top of the cirrus is small.

As an example, Fig. 1(a), (b) show the profiles of both the lidar received signal and the retrieved cirrus and aerosol extinction using Fernald's method [9]. The dot line in the Fig.1, and also in the following figures, represents the molecular extinction coefficient. It can be seen that the cirrus located at 10km has no effect on the retrieved aerosol extinction above the altitude.

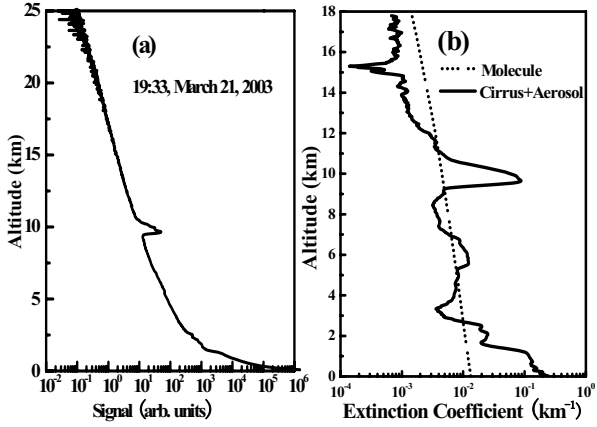


Fig. 1. profiles of the received signal (a) and the retrieved cirrus and aerosol extinction (b).

The so called differential zero-crossing method is used to retrieve cirrus base Z_b , peak Z_p and top Z_t [6,7]. That is the first derivative of the lidar received signal, $dP(z)/dz$, changes sign from negative to positive at the altitude of the cirrus base. A further change occurs at the altitude of the cirrus peak backscatter.

When the backscatter signals from the laser pulse above the top of the cirrus are well defined, the method locates Z_t at the altitude where $Z_t^2 P(Z_t) \leq Z_b^2 P(Z_b)$ [7].

The transmittance $T(Z_b, Z_t)$ and optical depth $\tau(Z_b, Z_t)$ of cirrus clouds are determined by using Wei-Nai Chen's method [8]:

$$T(Z_b, Z_t) = (P(Z_t^2) / P(Z_b^2))^{1/2} \quad (1)$$

$$\tau(Z_b, Z_t) = -\ln(T(Z_b, Z_t)) \quad (2)$$

4. RESULTS AND DISCUSSIONS

Fig. 2 shows time-series of range-corrected signals of cirrus observed by Mie lidar at Hefei on March 10, 2005.

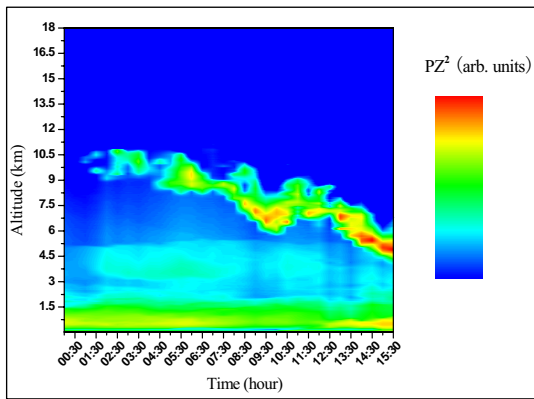


Fig. 2. Time-series of range-corrected signals of cirrus on March 10, 2005.

It clearly illustrates the development of cirrus structure over the lidar site. The initial thin cirrus located at

around 10 km were gradually descending with time. It fell to 5 km 15 hours later. Meanwhile the concentration of the cloud droplets in the central part of the cirrus was gradually increased with the decreasing height.

Fig.3 shows the location of the peak altitudes of the cirrus in relationship to the tropopause. Altitudes that correspond to -25°C are also presented in the figure.

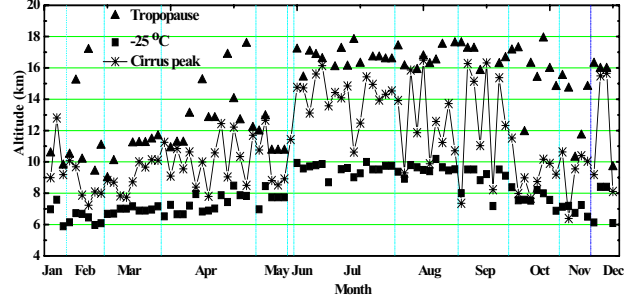


Fig. 3. The location of peak heights of the cirrus, the tropopause and altitudes with -25°C .

It indicates that all the peak altitudes of the cirrus were located between 6 km and 17 km. The mean value was 11.14 ± 2.69 km, which is well compared with 10.90 km determined by SAGE data at latitude of 25°N [5].

The most cirrus layers were situated in an air mass with a temperature colder than -25°C . The -25°C threshold, as determined from nearby radiosonde measurements, has been recognized as an indicator of cirrus [2].

The Figure also shows that even with large variability of both the peak altitude of the cirrus and the tropopause height, the former tended to track the latter.

Fig. 4 shows the thickness of cirrus as a function of month. It can be seen that the thickness range for most cirrus clouds was from hundreds of meters to 2 km. The mean value was 1.35 ± 0.66 km, which agrees quite well with the typical cirrus thickness of 1.5 km in the middle latitudes [5].

Comparing Fig.4 with Fig.3 indicates that higher cirrus clouds are thinner because their vertical extent is limited by the tropopause [4].

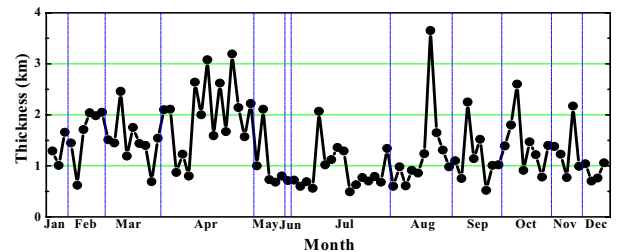


Fig. 4. Thickness of cirrus as a function as month.

Fig. 5 presents the optical depth of cirrus cloud as a function of month. Cirrus clouds with optical depth less

than 0.1 are known as thin cirrus. It is apparent that the most cirrus clouds observed by the lidar were thin cirrus. The cirrus clouds with optical depth larger than 0.1 appeared in spring months.

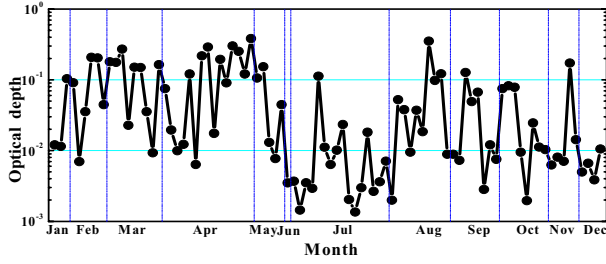


Fig. 5 presents the optical depth of cirrus cloud as a function of month.

In order to study the transport of the cirrus over the lidar site. Fig. 6 shows the wind speed and direction at the altitude of cirrus peak. It clearly illustrates that except summer, the cirrus clouds moved from west to east during the all other seasons.

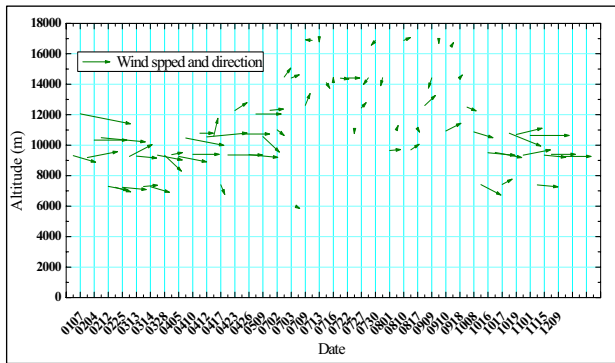


Fig. 6. Wind speed and direction at the altitude of cirrus peak over lidar site.

5. TRANSMITTANCE OF DISCONTINUOUS CIRRUS

Our routine lidar observations have shown that the aerosol extinction coefficient profiles often remain relatively stable during the nighttime in the absence of frontal activity. It might be associated with the stable vertical stratification at night.

We also have found that the cirrus clouds sometimes exist in discontinuous form.

Fig.7 gives an example. It presents two aerosol extinction coefficient profiles observed by lidar at 17:56 and 18:46 in the evening on Nov. 20, 2000. It is evident that the two profiles were shown to be nearly the same shape, except the cirrus existed in 10 km range at 17:56.

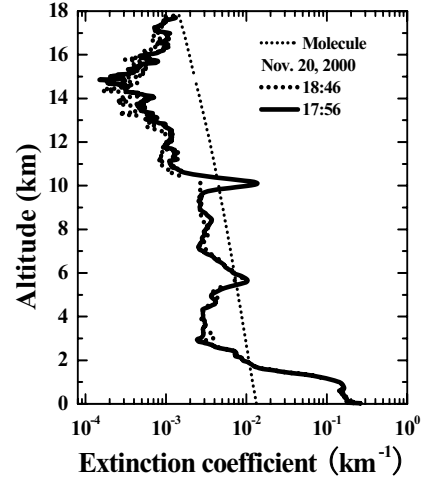


Fig.7. Lidar observed aerosol extinction profiles at 17:56 and 18:46 in the evening on Nov. 20, 2000.

In this condition, the transmittance of the cirrus can be retrieved by the following method:

If Z_1 is a certain altitude below the base of the cirrus, Z_2 is a certain altitude above the top of the cirrus. The lidar equations with cirrus can be written as:

$$P_1(z_1)Z_1^2 = C_1 \beta(z_1) T_1^2 \quad (3)$$

$$P_2(z_2)Z_2^2 = C_1 \beta(z_2) T_2^2$$

The lidar equation without cirrus can be written as:

$$P_1'(z_1)Z_1^2 = C_2 \beta'(z_1) T_1'^2 \quad (4)$$

$$P_2'(z_2)Z_2^2 = C_2 \beta'(z_2) T_2'^2$$

where $P(z)$ is signal received from altitude Z , C is the lidar system constant, $\beta(z)$ is the volume backscatter coefficient of the atmosphere, and T^2 is the round-trip transmittance of the atmosphere.

If the atmosphere keeps stable during the periods of lidar observations, at height Z_1 , $\beta(z)$ and T^2 with cirrus cloud have the following relation to the corresponding ones without cirrus:

$$\beta(z_1) = \beta'(z_1) \quad (5)$$

$$T_1^2 = T_1'^2 \quad (6)$$

and at the Z_2 , the relationship can be written as

$$\beta(z_2) = \beta'(z_2) \quad (7)$$

$$T_2^2 = T_2'^2 T_C^2 \quad (8)$$

Thus the transmittance of the cirrus T_C can be determined by

$$T_C = [(P_2(z^2)/P_2'(z^2)) \times (P_1'(z_1)/P_1(z_1))]^{1/2} \quad (9)$$

6. CONCLUSIONS

This paper has presented lidar observation results of high-altitude cirrus clouds over Hefei, the southeastern part of China. The following conclusions can be drawn on the basis of the lidar observed data sets:

- 1). The cirrus cloud layers were situated within 6 km and 17 km altitude range, where the air temperature was colder than -25°C.
- 2). The peak altitudes of the cirrus clouds were modulated by the altitude of the tropopause. The mean altitude was 11.14 ± 2.69 km.
- 3). The cirrus thickness range was from hundreds of meters to 2-km. The mean value was 1.35 ± 0.66 km. Higher cirrus clouds usually were thinner.
- 4). The optical depths of most lidar observed cirrus clouds were less than 0.1, a typical value for thin cirrus clouds.
- 5). The lidar observed results are compared with the ones reported in the existing literatures.
- 6). A method for determining the transmission of high-altitude cirrus clouds has been proposed. Further study about its feasibility will be made.

REFERENCES

1. Gabor Vali, Report of the Experts Meeting on Interaction between Aerosols and Clouds, WCRP-59, WMO/TD-No. 423, P26, 1991.
2. L. Goldfarb, et al. Cirrus climatological results from lidar measurements at OHP (44°N, 6°E), Geophysical Research Letter, Vol. 28, 1687-1690, 2001.
3. C. M. Platt, et al. The Experimental Cloud Lidar Pilot Study (ECLIPS) for Cloud-Radiation Research, Bulletin of the American Meteorological Society, Vol 75, 1635-1654, 1994.
4. Massimo Del Guasta, et al. One year of cloud lidar data from Dumont d'Urville (antarctica), J. Geophys. Res., Vol. 98, 18575-18587, 1993.
5. David R., et al. A summary of the physical properties of cirrus cloud, Journal of Applied Meteorology, Vol. 29, 970-978, 1990.
6. Stuart A. Yong, Analysis of lidar backscatter profiles in optically thin cloud, Appl.Opt., Vol. 34, 7019-7030, 1995.
7. Shiv R. Pal, et al. Automated method for lidar determination of cloud-base height and vertical extent, Appl. Opt., Vol. 31, 1488-1494, 1992.
8. Wei-Nai Chen, et al. Lidar ratio and depolarization ratio for cirrus clouds, Appl. Opt., Vol. 41, 6470-6476, 2002.
9. F. G. Fernald, Analysis of atmosphere lidar observation: some comments, Appl.Opt., Vol.23, 652-653, 1984.